

Reproduced by

Armed Services Technical Information Agency
DOCUMENT SERVICE CENTER

KNOTT BUILDING, DAYTON, 2, OHIO

AD -

2974

UNCLASSIFIED

AD No. 2974
ASTIA FILE COPY

OFFICE OF NAVAL RESEARCH

Contract N7onr-35810

NR-360-003

Technical Report No. 11

THE INTERACTION OF AN ACOUSTIC WAVE AND AN
ELASTIC SPHERICAL SHELL

by

~~Pauline Mann~~

GRADUATE DIVISION OF APPLIED MATHEMATICS

BROWN UNIVERSITY

PROVIDENCE, R. I.

February, 1953

The Interaction of an Acoustic Wave and an
Elastic Spherical Shell¹

By
Pauline Mann²

I. Introduction.

The problem to be considered here, that of a plane pressure wave impinging on a thin spherical shell, was suggested by G. F. Carrier in consequence of work previously done by him on a related problem [1]. (cf. also [6].)

An attempt had been made to determine the response to an incident acoustic wave of a thin elastic shell, in particular a cylindrical shell, taking into account both the incident and diffracted waves. The form of the functions dealt with in the analysis made it difficult to obtain accurate explicit results. If the obstacle is taken to be spherical in shape, we still have a fairly practical though highly simplified model of an actual physical structure; moreover, the problem becomes mathematically simpler, admitting of exact solutions for the deformation and accompanying strains in the elastic body. It was therefore decided to treat the case of the sphere in detail.

-
1. The results presented in this paper were obtained in the course of research sponsored by the Office of Naval Research under Contract N7onr - 35810 with Brown University.
 2. Research Associate, Brown University.

We will, as for the cylinder, deal with the linearized theory of wave propagation in a compressible fluid, and with small deflections of the shell.

II. Forced Vibrations of A Thin Spherical Shell.

We consider a closed shell of thickness h with $h \ll R$ where R is the radius of the middle surface. The motion of any closed oval¹ shell, in particular a spherical shell is, by a theorem of Jellett [2], primarily extensional. Therefore the general membrane theory of shells is applicable. If we locate the origin of our coordinate system at the center of the shell, and choose as the z -axis the direction of propagation of the incoming wave, then we have the additional simplification of symmetrical loading (c.f. Fig. 1). The equations of dynamic equilibrium for an element of shell may therefore be written [3]

$$\frac{\partial}{\partial \theta} (N_\theta R \sin \theta) - N_\varphi R \cos \theta - \rho h \frac{\partial^2 v}{\partial t^2} R^2 \sin \theta = 0 \quad (2.1)$$

$$N_\theta + N_\varphi = (s - \rho h \frac{\partial^2 w}{\partial t^2}) R = 0. \quad (2.2)$$

Here N_φ and N_θ are the normal forces/unit length acting on the sides of the element, s is the applied force (radial in direction), ρ is the shell density, and v and w are the tangential and radial components of the displacement.

To eliminate N_φ and N_θ from equations (2.1) and (2.2) we make use of Hooke's Law

1. Principle radii of curvature finite and of the same sign.

$$\varepsilon_{\theta\theta} = \frac{1}{Eh} (N_{\theta} - \nu N_{\varphi}) \quad (2.3)$$

$$\varepsilon_{\varphi\varphi} = \frac{1}{Eh} (N_{\varphi} - \nu N_{\theta}) \quad (2.4)$$

and the expressions for the strains in spherical coordinates

$$\varepsilon_{\theta\theta} = \frac{1}{R} \left[\frac{\partial v}{\partial \theta} + w \right] \quad (2.5)$$

$$\varepsilon_{\varphi\varphi} = \frac{1}{R} [v \cot \theta + w]. \quad (2.6)$$

Combining (2.3), (2.4), (2.5) and (2.6), we obtain N_{φ} and N_{θ} in terms of the displacements w and v

$$N_{\varphi} + N_{\theta} = \frac{Eh}{1-\nu} \left[\frac{v}{R} \cot \theta + 2 \frac{w}{R} + \frac{1}{R} \frac{\partial v}{\partial \theta} \right] \quad (2.7)$$

$$N_{\theta} - N_{\varphi} = - \frac{Eh}{1+\nu} \left[\frac{v}{R} \cot \theta - \frac{1}{R} \frac{\partial v}{\partial \theta} \right] \quad (2.8)$$

so that the equations of equilibrium become

$$\begin{aligned} \frac{Eh}{1-\nu^2} \left[v(-v + \frac{\partial w}{\partial \theta}) + \frac{\partial^2 v}{\partial \theta^2} + \frac{\partial w}{\partial \theta} + \frac{\partial v}{\partial \theta} \cot \theta - v \cot^2 \theta \right] \\ - \rho h \frac{\partial^2 v}{\partial t^2} R^2 = 0 \end{aligned} \quad (2.9)$$

$$\frac{Eh}{1-\nu} \left[v \cot \theta + 2w + \frac{\partial v}{\partial \theta} \right] - \left[s - \rho h \frac{\partial^2 w}{\partial t^2} \right] R^2 = 0. \quad (2.10)$$

An equation in v only can be easily obtained as follows. Consider the operator

$$M_0 = 2 + \frac{(1-\nu) R^2}{E} \frac{\partial^2}{\partial t^2}. \quad (2.11)$$

$M_0(w)$ is found from (2.10) to be equal to

$$-v \cot \theta - \frac{\partial v}{\partial \theta} + \frac{1-\nu}{Eh} R^2 s. \quad (2.12)$$

If M_0 is then applied to (2.9), and (2.12) substituted wherever $M_0(w)$ appears, a relation in v only results:

$$\begin{aligned}
 M_0(2.9) = & \frac{2(1-v^2)\rho R^2}{E} \frac{\partial^2 v}{\partial t^2} + \frac{(1-v^2)(1-v)\rho^2 R^4}{E^2} \frac{\partial^4 v}{\partial t^4} + 2vv \\
 & + \frac{v(1-v)\rho R^2}{E} \frac{\partial^2 v}{\partial t^2} - 2 \frac{\partial^2 v}{\partial \theta^2} - \frac{(1-v)\rho R^2}{E} \frac{\partial^4 v}{\partial t^2 \partial \theta^2} \\
 & + 2v \operatorname{ctn}^2 \theta + \frac{(1-v)\rho R^2}{E} \operatorname{ctn}^2 \theta \frac{\partial^2 v}{\partial t^2} - 2 \operatorname{ctn} \theta \frac{\partial v}{\partial \theta} \\
 & - \frac{(1-v)\rho R^2}{E} \frac{\partial^3 v}{\partial \theta \partial t^2} \operatorname{ctn} \theta - [1+v] \left[-\operatorname{ctn} \theta \frac{\partial v}{\partial \theta} + v \csc^2 \theta \right. \\
 & \left. - \frac{\partial^2 v}{\partial \theta^2} + \frac{(1-v)R^2}{Eh} \frac{\partial s}{\partial \theta} \right] = 0.
 \end{aligned} \tag{2.13}$$

A similar procedure² is used to arrive at an equation for w :

$$\begin{aligned}
 2w - \frac{1-v}{Eh} R^2 (s - \rho h \frac{\partial^2 w}{\partial t^2}) - \frac{2(1+v)\rho R^2}{E} \frac{\partial^2 w}{\partial t^2} + \frac{(1-v^2)\rho R^4}{E^2 h} \frac{\partial^2 s}{\partial t^2} \\
 - \frac{(1-v^2)\rho^2 R^4}{E^2} \frac{\partial^4 w}{\partial t^4} + \operatorname{ctn} \theta \frac{\partial w}{\partial \theta} + \frac{\partial^2 w}{\partial \theta^2} - \frac{R^2}{Eh} \operatorname{ctn} \theta \frac{\partial s}{\partial \theta} \\
 - \frac{R^2}{Eh} \frac{\partial^2 s}{\partial \theta^2} + \frac{R^2 \rho}{E} \operatorname{ctn} \theta \frac{\partial^3 w}{\partial t^2 \partial \theta} + \frac{\rho R^2}{E} \frac{\partial^4 w}{\partial t^2 \partial \theta^2} = 0.
 \end{aligned} \tag{2.14}$$

If we introduce the new variables

$$w^* = \frac{w}{R}; \quad v^* = \frac{v}{R}; \quad \tau^2 = \frac{t^2}{t_0^2} = \frac{Et^2}{R^2 \rho}; \quad s^* = \frac{s}{s_0} = \frac{Rs}{Eh}$$

then (13) and (14) reduce to the simpler non-dimensional forms

2. The operation $L_1(2.9) + L_2(2.10)$, where $L_1 = -(\operatorname{ctn} \theta + \frac{\partial}{\partial \theta})$ and $L_2 = 1 + \operatorname{ctn} \theta \frac{\partial}{\partial \theta} + \frac{\partial^2}{\partial \theta^2} - \frac{(1+v)\rho R^2}{E} \frac{\partial^2}{\partial t^2}$, gives the desired result.

$$\begin{aligned}
M(v^*) = & 2(1-v^2) \frac{\partial^2 v^*}{\partial \tau^2} + (1-v^2)(1-v) \frac{\partial^4 v^*}{\partial \tau^4} + 2vv^* + v(1-v) \frac{\partial^2 v^*}{\partial \tau^2} \\
& - 2 \frac{\partial^2 v^*}{\partial \theta^2} - (1-v) \frac{\partial^4 v^*}{\partial \tau^2 \partial \theta^2} + 2v^* \operatorname{ctn}^2 \theta + (1-v) \operatorname{ctn}^2 \theta \frac{\partial^2 v^*}{\partial \tau^2} \\
& - 2 \operatorname{ctn} \theta \frac{\partial v^*}{\partial \theta} - (1-v) \operatorname{ctn} \theta \frac{\partial^3 v^*}{\partial \theta \partial \tau^2} + [1+v] \left[\operatorname{ctn} \theta \frac{\partial v^*}{\partial \theta} \right. \\
& \left. - v^* \csc^2 \theta + \frac{\partial^2 v^*}{\partial \theta^2} \right] = (1-v^2) \frac{\partial s^*}{\partial \theta}
\end{aligned} \tag{2.15}$$

and

$$\begin{aligned}
L(w^*) = & \operatorname{ctn} \theta \left(\frac{\partial w^*}{\partial \theta} + \frac{\partial^3 w^*}{\partial \tau^2 \partial \theta} \right) + 2w^* + \frac{\partial^2 w^*}{\partial \theta^2} + \frac{\partial^4 w^*}{\partial \tau^2 \partial \theta^2} \\
& - (1-v^2) \frac{\partial^4 w^*}{\partial \tau^4} + (1-v) \frac{\partial^2 w^*}{\partial \tau^2} - 2(1+v) \frac{\partial^2 w^*}{\partial \tau^2} \\
= & \operatorname{ctn} \theta \frac{\partial s^*}{\partial \theta} - (1-v^2) \frac{\partial^2 s^*}{\partial \tau^2} + \frac{\partial^2 s^*}{\partial \theta^2} + (1-v)s^*.
\end{aligned} \tag{2.16}$$

III. Acoustic Wave Propagation.

As in the cylindrical case [1] we have the acoustic wave equation

$$\Delta \varphi - \lambda^2 \varphi_{\tau\tau} = 0 \tag{3.1}$$

where φ is the velocity potential, $\Delta \varphi$ is the Laplacian in spherical coordinates and $\lambda^2 = \frac{R^2}{t_0^2 c^2} = \frac{E}{\rho c^2}$ (c^2 is the acoustic speed of the fluid.) The pressure perturbation p is again given by

$$\begin{aligned}
p = & -p^* \varphi_{,\tau}(r, \theta, \tau) \\
p^* = & \frac{\rho_f R^2}{t_0^2} = \frac{\rho_f E}{\rho}
\end{aligned} \tag{3.2}$$

where ρ_f is the fluid density. The applied stress s of (2.2) must of course be the same as the acoustic pressure p at the surface of the sphere. We have in fact

$$s^* = -\frac{p}{s_0} = \frac{p^*}{s_0} \varphi_{,\tau}(1, \theta, \tau) = \frac{\rho_f R}{\rho h} \varphi_{,\tau}(1, \theta, \tau) = \beta \varphi_{,\tau}(1, \theta, \tau).$$

IV. The Interaction Problem.

We now pose the following problem. An incoming plane wave, φ_0 , obeying (3.1) impinges on an elastic spherical shell causing it to vibrate according to (2.15) and (2.16). The vibrating body acts as a scatterer and, to a lesser extent, as a radiator. The outgoing waves (scattered and radiated) also obeying (3.1), in turn influence the nature of the vibrations. At the surface of the shell, the radial velocity of the fluid, $\varphi_r(1, \theta, \tau)$, must be equal to the radial velocity of the shell, $w_\tau^*(\theta, \tau)$. We wish to determine the motion of the sphere and the pressure distribution associated with the incoming and outgoing waves.

The pressure associated with the incident wave is taken to be [1]

$$p = \begin{cases} Q_0 e^{\delta(z-\tau/\lambda)} & z \leq \tau/\lambda \\ 0 & z > \tau/\lambda \end{cases} \quad (4.1)$$

so that the initial velocity potential is

$$\varphi_0 = \begin{cases} \frac{Q_0 \lambda}{p^* \delta} e^{\delta(z-\tau/\lambda)} - \frac{Q_0 \lambda}{p^* \delta} & z \leq \tau/\lambda \\ 0 & z > \tau/\lambda. \end{cases} \quad (4.2)$$

For simplicity let

$$\begin{aligned} \varphi_0 &= \frac{Q_0}{p^*} \psi^0, & \varphi &= \frac{Q_0}{p^*} (\psi^0 + \psi) = \frac{Q_0}{p^*} \chi \\ w^* &= \frac{Q_0}{p^*} W, & v^* &= \frac{Q_0}{p^*} V. \end{aligned} \quad (4.3)$$

Then our boundary value problem is defined by the following set of equations:³

$$L(W) = \beta[\chi'_{\tau}(1, \theta, \tau) \cot \theta - (1-v^2)\chi_{\tau\tau}(1, \theta, \tau) + \chi''_{\tau}(1, \theta, \tau) + (1-v)\chi_{\tau}(1, \theta, \tau)] \quad (4.4)$$

$$M(V) = \beta(1-v^2)\chi'_{\tau}(1, \theta, \tau) \quad (4.5)$$

$$\Delta\psi - \lambda^2\psi_{\tau\tau} = 0 \quad (4.6)$$

$$W_{\tau}(\theta, \tau) = \chi_r(1, \theta, \tau) \quad [\text{Boundary Condition}] \quad (4.7)$$

$$\psi_0 = \begin{cases} \frac{\lambda}{\delta} e^{\delta(z-\tau/\lambda)} - \frac{\lambda}{\delta} & z \leq \tau/\lambda \\ 0 & z > \tau/\lambda \end{cases} \quad (4.8)$$

These equations will be more easily handled if Fourier transforms are first introduced to eliminate the time dependence. Denote the transform of a function F by \bar{F} . Then F and \bar{F} are related by:

$$\bar{F}(r, \theta, \eta - i\alpha) = \int_{-\infty}^{+\infty} F(r, \theta, \tau) e^{-\alpha\tau} e^{-i\eta\tau} d\tau \quad (4.9a)$$

where α is any positive real number.

$$F(r, \theta, \tau) = \frac{1}{2\pi} e^{\alpha\tau} \int_{-\infty}^{+\infty} \bar{F}(r, \theta, \eta - i\alpha) e^{i\eta\tau} d\eta$$

or, letting $\eta - i\alpha = \xi$

$$F(r, \theta, \tau) = \frac{1}{2\pi} \int_{-i\alpha - \infty}^{-i\alpha + \infty} \bar{F}(r, \theta, \xi) e^{i\xi\tau} d\xi. \quad (4.9b)$$

This generalized definition of the Fourier transform has been used because the usual definition, $F(r, \theta, \eta) = \int_{-\infty}^{+\infty} F(r, \theta, \tau) e^{-i\eta\tau} d\tau$,

3. The operators L and M which appear here are those given in (2.15) and (2.16).

fails in the case of the function χ .⁴

Applying (4.9a) to (3.4) through (3.8) we obtain

$$\bar{L}(\bar{W}) = i\beta\xi [\bar{\chi}' \operatorname{ctn} \theta + \bar{\chi}''(1, \theta, \xi) + (1-v)\bar{\chi} + \xi^2(1-v^2)\bar{\chi}] \quad (4.10)$$

where

$$\bar{L} = \left\{ \operatorname{ctn} \theta \left(\frac{\partial}{\partial \theta} - \xi^2 \frac{\partial}{\partial \theta} \right) + 2 + \frac{\partial^2}{\partial \theta^2} - \xi^2 \frac{\partial^2}{\partial \theta^2} - (1-v^2)\xi^4 - (1-v)\xi^2 + 2(1+v)\xi^2 \right\}$$

$$\bar{M}(\bar{V}) = i\beta\xi (1-v^2)\bar{\chi}' \quad (4.11)$$

where

$$\bar{M} = \left\{ -2(1-v^2)\xi^2 + (1-v^2)(1-v)\xi^4 + 2v - v(1-v)\xi^2 - 2 \frac{\partial^2}{\partial \theta^2} + (1-v)\xi^2 + 2 \operatorname{ctn}^2 \theta - (1-v)\xi^2 \operatorname{ctn}^2 \theta - 2 \operatorname{ctn} \theta \frac{\partial}{\partial \theta} + (1-v)\xi^2 \operatorname{ctn} \theta \frac{\partial}{\partial \theta} + (1+v)(\operatorname{ctn} \theta \frac{\partial}{\partial \theta} - \csc^2 \theta + \frac{\partial^2}{\partial \theta^2}) \right\}$$

$$\Delta \bar{\psi} + \lambda^2 \xi^2 \bar{\psi} = 0 \quad (4.12)$$

$$i\xi \bar{W}(\theta, \xi) = \bar{\chi}_r(1, \theta, \xi) \quad (4.13)$$

$$\bar{\psi}^0 = \frac{-e^{-i\lambda z \xi}}{i\xi(\delta/\lambda + i\xi)} = -f(\xi)e^{-i\lambda r \xi \cos \theta} \quad (4.14)$$

It can be shown, using the method of separation of variables on (4.12), that $\bar{\psi}$ is of the form

$$r^{-1/2} [J_{n+\frac{1}{2}}(\lambda \xi r) + cY_{n+\frac{1}{2}}(\lambda \xi r) P_n(\cos \theta)].$$

4. It should be noted that for the functions we are interested in, the tendency of the integrand in (4.9a) to become infinite for large negative τ is only apparent. Actually, $\bar{\psi}^0 = 0$ for $-\infty < \tau/\lambda < z$; and W , V , and ψ are zero until the wave hits the shell, i.e. for $-\infty < \tau/\lambda < -1$, so that integral of (4.9a) always exists.

Since the waves associated with $\bar{\psi}$ must be outwardly moving, take $C = -i$ and write:

$$\bar{\psi} = \sum_{n=0}^{\infty} A_n(\xi) h_n^{(2)}(\lambda \xi r) P_n(\cos \theta) \quad (4.15)$$

where

$$h_n^{(2)}(\lambda \xi r) = \left(\frac{\pi}{\lambda \xi r} \right)^{1/2} [J_{n+\frac{1}{2}}(\lambda \xi r) - iY_{n+\frac{1}{2}}(\lambda \xi r)] .$$

$\bar{\psi}_0$ may be expanded similarly:

$$\begin{aligned} \bar{\psi}^0(r, \theta, \xi) &= -f(\xi) \sum_{n=0}^{\infty} (2n+1)(-1)^n j_n(\lambda \xi r) P_n(\cos \theta) \quad (4.16) \\ &= \sum_{n=0}^{\infty} B_n(\xi) j_n(\lambda \xi r) P_n(\cos \theta) \end{aligned}$$

where

$$j_n(\lambda \xi r) = \left(\frac{\pi}{\lambda \xi r} \right)^{1/2} J_{n+\frac{1}{2}}(\lambda \xi r) .$$

From the work of Lamb [4] we know that the complete solutions for \bar{W} and \bar{V} may be written:

$$\bar{W}(\theta, \xi) = \sum_{n=0}^{\infty} \bar{W}_n(\xi) P_n(\cos \theta) \quad (4.17)$$

$$\bar{V}(\theta, \xi) = - \sum_{n=0}^{\infty} \bar{V}_n(\xi) P_n^1(\cos \theta) = - \sum_{n=0}^{\infty} \bar{W}_n P_n'(\cos \theta) \sin \theta. \quad (4.18)$$

Substituting these expressions into (4.10), (4.11) and (4.13), we get three algebraic equations for the three unknowns \bar{W}_n , \bar{V}_n and A_n .

$$\begin{aligned} &[(1-\xi^2)(n^2+n) - 2 + (1-v^2)\xi^4 + (1-v)\xi^2 - 2(1+v)\xi^2] \bar{W}_n \\ &= -i\beta\xi [(1-v) + (1-v^2)\xi^2 - (n^2+n)] [A_n h_n^{(2)}(\lambda \xi) + B_n j_n(\lambda \xi)] \quad (4.19) \end{aligned}$$

$$\begin{aligned} &[2(1+v)\xi^2 - (1-v^2)\xi^4 + v\xi^2 + 1 + (n+n^2-1)(\xi^2-1)] \bar{V}_n \\ &= -i\beta\xi(1+v) [A_n h_n^{(2)}(\lambda \xi) + B_n j_n(\lambda \xi)] \quad (4.20) \end{aligned}$$

$$\lambda \xi B_n(\xi)' \big|_{j_n} (\lambda \xi) + \lambda \xi A_n(\xi) h_n^{(2)'} (\lambda \xi) = i \xi W_n \quad (4.21)$$

These are readily solved to give:

$$W_n = \frac{(2n+1)(-1)^n C_2}{\lambda \xi (i \xi)^2 \left(\frac{\delta}{\lambda} + i \xi \right) [C_1 \lambda h_n^{(2)'} + i C_2 h_n^{(2)}]} \quad (4.22)$$

$$V_n = - \frac{(2n+1)(-1)^n \beta (1+\nu)}{\lambda \xi (i \xi) \left(\frac{\delta}{\lambda} + i \xi \right) [C_1 \lambda h_n^{(2)'} + i C_2 h_n^{(2)}]} \quad (4.23)$$

$$A_n = - \frac{1}{2} \left[1 + \frac{C_1 \lambda h_n^{(1)'} + i C_1 h_n^{(1)}}{C_1 \lambda h_n^{(2)'} + i C_2 h_n^{(2)}} \right] \frac{1}{\xi^2} (2n+1)(-1)^n \quad (4.24)$$

where

$$C_1 = (1-\xi^2)(n^2+n) - 2 + (1-\nu^2)\xi^4 + (1-\nu)\xi^2 - 2(1+\nu)\xi^2$$

$$C_2 = i \beta \xi [(1-\nu) + (1-\nu^2)\xi^2 - (n^2+n)].$$

The quantities of physical interest to us are the stresses and radial acceleration associated with each vibrational mode, and the total pressure distribution. These can all be found at least in principle from (4.22), (4.23), (4.24), (4.15) and the inversion formula (4.9b).

V. Numerical results for the shell.

The transforms of the stress components will all be linear combinations of \bar{W}_n and \bar{V}_n (in general, $g_1(\theta)\bar{W}_n + g_2(\theta)\bar{V}_n$), and the transforms of the radial accelerations will be $-\xi^2 \bar{W}_n$. From (4.22) and (4.23) we see that these expressions are regular in ξ except for a finite number of poles. The theorem of residues can therefore be used to evaluate the integral of (4.9b).

The computation will be carried out in detail for the three lowest modes. The parameters will be taken as

$$\beta = 17, \delta = 0, \lambda^2 = \frac{25}{3}, \quad \nu = .3$$

the values appropriate to a wave of infinite length impinging on a steel shell in water.

Zeroth Mode. For this mode, the motion of the sphere is very simple, consisting of uniform (θ - independent) expansions and contractions of varying amplitude and period.

The stresses, N_φ and N_θ , are given by

$$N_\varphi = N_\theta = \frac{Eh}{1-\nu} \frac{w_0}{R} = \frac{Q_0 R}{(1-\nu)\beta} w_0.$$

$$w_0 = -\frac{1}{2\pi} \int_{-i\alpha\lambda}^{-i\alpha\lambda+\infty} \frac{(1-\nu)k^2 \beta e^{i\zeta(\frac{\tau}{\lambda}+1)} d\zeta}{2\zeta(\zeta^3 - k^2\zeta - 18i\zeta^2 + ik^2)}$$

$$\text{Here } k^2 = \frac{2\lambda^2}{1-\nu}; \quad \zeta = \lambda\xi.$$

The integrand is regular except for poles at

$$\zeta = 0, \quad 16.58i, \quad \pm 1 + .71i$$

with residues respectively of

$$1, \quad .0060e^{-16.58(\frac{\tau}{\lambda}+1)}, \quad \text{and} \quad -1.2818e^{-.71(\frac{\tau}{\lambda}+1)} \sin(\frac{\tau}{\lambda} + 1.89).$$

Jordan's lemma can be adapted to give

$$w_0 = \frac{-(1-\nu)\beta}{2} [1.00 - 1.2818e^{-.71(\frac{\tau}{\lambda}+1)} \sin(\frac{\tau}{\lambda} + 1.89) - 0.0060e^{-16.58(\frac{\tau}{\lambda}+1)}]. \quad (5.1)$$

A plot of $-2N_\varphi/RQ_0$ appears in Figure 2. ⁵

5. These scales will also be used in plotting the 1st and 2nd modes. The reason for their choice will become clear on page 18.

The radial acceleration is found directly from (5.1) to be

$$\frac{\partial^2 w_0}{\partial \tau^2} = \frac{Q_0 R^2}{Eh\beta} \frac{\partial^2 w_0}{\partial \tau^2} = - \frac{Q_0 R^2}{4Eh} \left\{ e^{-.71(\frac{\tau}{\lambda} + 1)} \left[0.0941 \sin \left(\frac{\tau}{\lambda} + 1.89 \right) + 0.2697 \cos \left(\frac{\tau}{\lambda} + 1.89 \right) \right] - 0.2427^{-16.58(\frac{\tau}{\lambda} + 1)} \right\}. \quad (5.2)$$

The plot of $-\frac{4Eh}{Q_0 R^2} \frac{\partial^2 w}{\partial \tau^2} \Big|_0$ appears in Figure 5.⁵

There is an alternative to the computational scheme we have used, in which the integrand is expanded in a power series about infinity and the series integrated term by term. Since there was a possibility that it might prove simpler, this was tried out, the zeroth mode acceleration being taken as a test case.

$$\begin{aligned} \frac{\partial^2 w_0}{\partial \tau^2} &= \frac{1}{2\pi} \int_{-i\lambda + \infty}^{-i\lambda - \infty} \frac{\beta \zeta e^{i\zeta(\frac{\tau}{\lambda} + 1)} d\zeta}{\zeta^3 - k^2 \zeta - 18i\zeta^2 + ik^2} \\ - \frac{4Ehw_0}{Q_0 R^2} \Big|_0 &= - \frac{4}{2\pi} \int_{\infty}^{\infty} e^{i\zeta(\frac{\tau}{\lambda} + 1)} \left[\zeta^{-2} + 18i\zeta^{-3} \right. \\ &\quad \left. - 299\zeta^{-4} - 4957i\zeta^{-5} + 8220i\zeta^{-6} + \dots \right] d\zeta \\ &= \left[\left(\frac{\tau}{\lambda} + 1 \right) - 36 \left(\frac{\tau}{\lambda} + 1 \right)^2 + \frac{2}{3} (299) \left(\frac{\tau}{\lambda} + 1 \right)^3 + \dots \right]. \quad (5.3) \end{aligned}$$

The results, which appear in Table 1, demonstrate the impracticality of this new procedure. It is apparent that at least 12 terms are needed to find only the first maximum to within 10%

⁵ These scales will also be used in plotting the 1st and 2nd modes. The reason for their choice will become clear on page 18.

First Mode

The stress components here are

$$\begin{aligned}
 N_{\varphi} = N_{\theta} &= \frac{Eh}{1-\nu} \left[\frac{w}{R} + \frac{1}{R} \frac{\partial v}{\partial \theta} \right]_1 = \frac{Eh}{(1-\nu)} \left[\frac{w}{R} + \frac{\nu \cot \theta}{R} \right]_1 \\
 &= \frac{Q_0 R}{(1-\nu)\beta} \left[W + \frac{\partial V}{\partial \theta} \right]_1 = \frac{Q_0 R}{(1-\nu)\beta} [W_1 - V_1] \cos \theta. \\
 W_1 - V_1 &= -\frac{3\beta}{2\pi i} \int_{-i\alpha\lambda-\infty}^{-i\alpha\lambda+\infty} \frac{2e^{i\zeta \frac{\tau}{\lambda}} d\zeta}{21\zeta^4 + 38\zeta^3 - 113i\zeta^2 - 575\zeta + 575i}
 \end{aligned}$$

The integrand has poles at

$$\zeta = 1.171, \quad 16.581, \quad \text{and} \quad \pm 3.81 + 0.645i.$$

On computing the residues we obtain

$$\begin{aligned}
 W_1 - V_1 &= 1.9666e^{-1.17(\frac{\tau}{\lambda} + 1)} - 0.1076e^{-16.58(\frac{\tau}{\lambda} + 1)} \\
 &\quad - 1.8488e^{-0.625(\frac{\tau}{\lambda} + 1)} \sin \left[3.811(\frac{\tau}{\lambda} + 1) + 1.479 \right]. \quad (5.4)
 \end{aligned}$$

Figure 3 shows a plot of $-2N_{\varphi}/RQ_0$ at the point $\theta = \pi$.

The radial acceleration is found most easily by inverting the transform, $-\zeta^2 \bar{W}_1 \cos \theta$.

$$\begin{aligned}
 \left. \frac{\partial^2 w}{\partial \tau^2} \right]_1 &= \frac{Q_0 R^2}{Eh\beta} \left. \frac{\partial^2 W}{\partial \tau^2} \right]_1 = \frac{Q_0 R^2}{Eh\beta} \frac{\partial^2 W_1}{\partial \tau^2} \cos \theta \\
 \frac{\partial^2 W_1}{\partial \tau^2} &= \frac{1}{2\pi i} \int_{-i\alpha\lambda-\infty}^{-i\alpha\lambda+\infty} \frac{(102\zeta^2 - 1275)e^{i\zeta(\frac{\tau}{\lambda} + 1)} d\zeta}{21\zeta^4 + 38\zeta^3 - 113i\zeta^2 - 575\zeta + 575i} \\
 &= 1.064e^{-0.625(\frac{\tau}{\lambda} + 1)} \sin \left[2.72 + 3.8109(\frac{\tau}{\lambda} + 1) \right] \\
 &\quad - 3.5335e^{-16.58(\frac{\tau}{\lambda} + 1)} + 3.1171e^{-1.17(\frac{\tau}{\lambda} + 1)} \quad (5.5)
 \end{aligned}$$

$-\frac{4Eh}{Q_0 R^2} \left[\frac{\partial^2 w}{\partial \tau^2} \right]_1$ is plotted for $\theta = \pi$ in Figure 6.

Second Mode.

In general, the two tangential stress components are not equal to each other for this mode. We have, in fact,

$$N_\theta = \frac{Eh}{1-\nu^2} [\epsilon_\theta + \nu \epsilon_\varphi], \quad N_\varphi = \frac{Eh}{1-\nu^2} [\epsilon_\varphi + \nu \epsilon_\theta],$$

where

$$\epsilon_\theta = \frac{1}{R} \left[w + \frac{\partial v}{\partial \theta} \right]_2 = \frac{Q_0 R}{Eh\beta} \left[w + \frac{\partial v}{\partial \theta} \right]_2 = \frac{Q_0 R}{Eh\beta} \left[3 \cos^2 \theta (-2V_2 + \frac{1}{2}W_2) + (3V_2 - \frac{1}{2}W_2) \right]$$

$$\begin{aligned} \epsilon_\varphi &= \frac{1}{R} \left[w + v \cot \theta \right]_2 = \frac{Q_0 R}{Eh\beta} \left[w + v \cot \theta \right]_2 \\ &= \frac{Q_0 R}{Eh\beta} \left[3 \cos^2 \theta (-V_2 + \frac{1}{2}W_2) - \frac{1}{2}W_2 \right]. \end{aligned}$$

$$W_2 = \frac{1}{2\pi} \int_{-i\alpha\lambda-\infty}^{-i\alpha\lambda+\infty} \frac{[676.8125\zeta^3 - 34491.40625\zeta] e^{i\zeta(\frac{\pi}{\lambda}+1)} d\zeta}{D}$$

$$V_2 = -\frac{1}{2\pi} \int_{-i\alpha\lambda-\infty}^{-i\alpha\lambda+\infty} \frac{8460.15625\zeta e^{i\zeta(\frac{\pi}{\lambda}+1)} d\zeta}{D}$$

where

$$\begin{aligned} D = &-.91\zeta^7 + 19.11 i\zeta^6 + 123.725\zeta^5 - 1119.475 i\zeta^4 - 3292.5\zeta^3 + \\ &+ 4212.25 i\zeta^2 + 2756.25\zeta - 2756.25i \end{aligned} \quad (5.6)$$

The denominators have seven zeros:

$$16.54 i, \pm 7.35 + 0.43 i, \pm 0.86 + 1.79 i, \pm 0.92 + 0.007 i.$$

The theorem of residues gives

$$\begin{aligned}
 W_2 = & 0.213e^{-16.54(\frac{\tau}{\lambda} + 1)} - 2e^{-0.43(\frac{\tau}{\lambda} + 1)} \left\{ 0.0426 \left[\sin 7.3483(\frac{\tau}{\lambda} + 1) \right] \right. \\
 & - 0.0254 \cos \left[7.3483(\frac{\tau}{\lambda} + 1) \right] \left. \right\} + 2e^{-1.79(\frac{\tau}{\lambda} + 1)} \left\{ 12.2253 \sin \left[0.8578(\frac{\tau}{\lambda} \right. \right. \\
 & + 1) \left. \right] + 2.8318 \cos \left[0.8578(\frac{\tau}{\lambda} + 1) \right] \left. \right\} - 2e^{-0.007(\frac{\tau}{\lambda} + 1)} \left\{ 3.6145 \right. \\
 & \sin \left[0.9242(\frac{\tau}{\lambda} + 1) \right] + 2.9634 \cos \left[0.9242(\frac{\tau}{\lambda} + 1) \right] \left. \right\} \quad (5.7)
 \end{aligned}$$

$$\begin{aligned}
 V_2 = & 0.0082e^{-16.54(\frac{\tau}{\lambda} + 1)} - 2e^{0.43(\frac{\tau}{\lambda} + 1)} \left\{ 0.0102 \sin \left[7.35(\frac{\tau}{\lambda} + 1) \right] \right. \\
 & + 0.0888 \cos \left[7.35(\frac{\tau}{\lambda} + 1) \right] \left. \right\} + 2e^{-1.79(\frac{\tau}{\lambda} + 1)} \left\{ 2.8117 \left[\sin 0.8578(\frac{\tau}{\lambda} \right. \right. \\
 & + 1) \left. \right] + 0.8242 \cos \left[0.8578(\frac{\tau}{\lambda} + 1) \right] \left. \right\} - 2e^{-0.007(\frac{\tau}{\lambda} + 1)} \left\{ 0.9015 \right. \\
 & \cdot \sin \left[0.9242(\frac{\tau}{\lambda} + 1) \right] + 0.7395 \cos \left[0.9242(\frac{\tau}{\lambda} + 1) \right] \left. \right\}. \quad (5.8)
 \end{aligned}$$

At $\Theta = \pi$ where the greatest stresses occur, $N_\Theta = N_\varphi =$

$\frac{Q_0 R}{(1-\nu)\beta} (W_2 - 3V_2)$. A plot of $-\frac{2N_\varphi}{Q_0 R}$ for $\Theta = \pi$ appears in Figure 4.

The radial acceleration is given by

$$\left[\frac{\partial^2 w}{\partial \tau^2} \right]_2 = \frac{Q_0 R^2}{E h \beta} \left[\frac{\partial^2 W}{\partial \tau^2} \right]_2 = \frac{Q_0 R^2}{E h \beta} \frac{\partial^2 W_2}{\partial \tau^2} \left(\frac{3 \cos 2\Theta + 1}{4} \right)$$

$$\frac{\partial^2 W_2}{\partial \tau^2} = - \frac{1}{2\pi\lambda^2} \int_{-i\alpha\lambda-\infty}^{-i\alpha\lambda+\infty} \frac{[676.8125\zeta^5 - 34491.40625\zeta^3] e^{i\zeta(\frac{\tau}{\lambda} + 1)} d\zeta}{D}$$

where D is given in (5.6).

$$\begin{aligned}
 \frac{\partial^2 W_2}{\partial \tau^2} = & 6.6576 e^{-16.54(\frac{\tau}{\lambda} + 1)} + e^{-0.43(\frac{\tau}{\lambda} + 1)} \left\{ 0.564 \sin \left[7.3483(\frac{\tau}{\lambda} + \right. \right. \\
 & + 1) \left. \right] - 0.2457 \cos \left[7.3483(\frac{\tau}{\lambda} + 1) \right] \left. \right\} + e^{-1.79(\frac{\tau}{\lambda} + 1)} \left\{ 8.939 \sin \left[0.8578 \right. \right. \\
 & \cdot (\frac{\tau}{\lambda} + 1) \left. \right] - 6.9956 \cos \left[0.8578(\frac{\tau}{\lambda} + 1) \right] \left. \right\} + e^{-0.007(\frac{\tau}{\lambda} + 1)} \\
 & \left\{ 0.6982 \sin \left[0.9242(\frac{\tau}{\lambda} + 1) \right] + 0.5966 \cos \left[0.9242(\frac{\tau}{\lambda} + 1) \right] \right\}. \quad (5.9)
 \end{aligned}$$

$-\frac{4Eh}{Q_0 R^2} \frac{\partial^2 w}{\partial \tau^2} \Big]_2$ is plotted for $\theta = \pi$ in Figure 7.

If we examine Figures 2, 3, and 4 it becomes evident that the stresses in the lowest mode are very much greater than those of the 1st and 2nd modes, and very likely those of the higher modes as well. In this connection it should be recalled that the plots in Figures 3 and 4, which were made for $\theta = \pi$, show the largest stresses which can occur in the first and second modes at any time. We may therefore consider the resultant stresses in the sphere to be predominantly those of the zeroth mode.

The case of the acceleration is not so simple. A picture of the total acceleration cannot be gained by looking at the lower modes. In fact, it would seem from Figures 5, 6, and 7, that the series, $\sum_{n=0}^{\infty} \frac{\partial^2 w_n}{\partial \tau^2}$ does not represent the total acceleration for all τ . The rate of change of radial acceleration is very great for the first three modes at $\tau/\lambda = -1$, $\theta = \pi$; probably the total radial acceleration as summed mode by mode will be discontinuous at $\tau = -\lambda$, $\theta = \pi$. This indicates that $\sum_{n=0}^{\infty} \frac{\partial^2 w_n}{\partial \tau^2}$ does not converge uniformly, and therefore that $\frac{\partial^2 w}{\partial \tau^2} \neq \sum_{n=0}^{\infty} \frac{\partial^2 w_n}{\partial \tau^2}$. This difficulty, associated with the use of the series expansion as a method of solution, will be encountered again in Section VI when we discuss the resultant pressure distribution. By anticipating the results of that section, we can find the initial value of $\frac{\partial^2 w}{\partial \tau^2}$ at $\theta = \pi$.

Equation (2.2) gives, for $\tau/\lambda = -1$

$$S = \rho h \frac{\partial^2 w}{\partial \tau^2} = \frac{\rho h}{R^2 \rho} \frac{\partial^2 w}{\partial \tau^2}$$

$$\frac{-4S}{Q_0} = - \frac{4Eh}{Q_0 R^2} \frac{\partial^2 w}{\partial \tau^2}.$$

Taking

$$S = -2Q_0 \quad ((6.9), \theta = \pi)$$

we have

$$- \frac{4Eh}{Q_0 R^2} \frac{\partial^2 w}{\partial \tau^2} = 8.$$

Thus, while we can obtain a very good approximation of the stresses by considering only the lowest mode, the same is definitely not true of the acceleration. The actual initial acceleration is about 40 times as great as the maximum acceleration in the zeroth mode. The agreement obtained by considering the first and second modes along with the zeroth is not appreciably better; the results still differ by more than a factor of 6.

Quasi-Static Case.

It is of interest to compare the hoop stresses we have obtained, as represented by those of the zeroth mode, with the stresses for the quasi-static case; i.e. for the case in which the sphere is taken to be rigid and scattering is neglected.

Since the effects of only the incident wave are considered, we have for the pressure at time t

$$\text{pressure} = \begin{cases} \frac{Q_0 2\pi R(tc+R)}{4\pi R^2} = \frac{Q_0 \left(\frac{t}{\lambda} + 1\right)}{2} & -1 \leq \frac{t}{\lambda} \leq 1. \\ Q_0 & +1 \leq \frac{t}{\lambda} < \infty. \end{cases}$$

The stresses are given by

$$N_{\theta} = N_{\varphi} = \begin{cases} -\frac{RQ_0(\frac{\tau}{\lambda} + 1)}{4} & -1 \leq \frac{\tau}{\lambda} + 1 \\ -\frac{RQ_0}{2} & +1 < \frac{\tau}{\lambda} < \infty \end{cases}$$

$-\frac{2N_{\varphi}}{RQ_0}$ appears as the dotted line in Figure 2, where it can be seen that the very simple quasi-static case approximates the more exact dynamic case very closely. The stress developments, while slightly out of phase, are essentially parallel with a difference in maxima of only 1%.

For $-1 \leq \tau/\lambda \leq 1$, there will be an unbalanced force, due to the incident wave, acting on the sphere. This will result in an acceleration of the rigid body in the z-direction. The magnitude of the force is

$$\begin{aligned} \int_{\theta_0}^{\pi} \int_0^{2\pi} R^2 Q_0 \cos \theta \sin \theta d\varphi &= Q_0 \pi R^2 \sin^2 \theta_0 \\ &= Q_0 \pi [R^2 - (tc)^2] \\ &= Q_0 \pi R^2 [1 - (\tau/\lambda)^2]. \end{aligned}$$

Therefore

$$4\pi R^2 h \rho \frac{\partial^2 z}{\partial \tau^2} = Q_0 \pi R^2 [1 - (\frac{\tau}{\lambda})^2]$$

$$\frac{4Eh}{R^2} \frac{\partial^2 z}{\partial \tau^2} = Q_0 [1 - (\frac{\tau}{\lambda})^2]$$

$$\frac{4Eh}{Q_0 R^2} \frac{\partial^2 z}{\partial \tau^2} = [1 - (\frac{\tau}{\lambda})^2].$$

This has been plotted for purposes of comparison in Figures 5, 6, and 7 (dotted curves).

The maximum acceleration in the zeroth mode is only one fifth that of the rigid sphere. The resemblance is greater for the first mode, where the two significant maxima occur within the time $|\frac{\tau}{\lambda}| < 1$, the larger being one half that of the rigid sphere. In the second mode where we begin to have large negative accelerations, there is considerable difference in form between the dynamic and quasi-static cases although the maximum positive acceleration of the former, .7, has moved still closer to the rigid body value of 1.

This value of 1 is, we recall, very much smaller than the maximum of the total radial acceleration for the dynamic case (p. 17).

VI. Resultant pressure distribution.

From (3.2), (4.2), (4.15), (4.24) and (4.9b) the total pressure is known to be:

$$\begin{aligned}
 P_{\text{total}} &= P_I(\text{Incident}) + P_{II} = -p^* \varphi_\tau = -Q_0 \chi_\tau \\
 &= Q_0 - \frac{iQ_0}{2\pi} \int_{-i\alpha-\infty}^{-i\alpha+\infty} e^{i\xi\tau} \bar{\psi}_\xi d\xi \\
 &= Q_0 + \frac{iQ_0}{2\pi} \int_{-i\alpha+\infty}^{-i\alpha-\infty} \xi e^{i\xi\tau} \sum \frac{(-1)^n (2n+1)}{2\xi^2} h_n^{(2)}(\lambda\xi r) \left[1 + \right. \\
 &\quad \left. + \frac{C_1 \lambda h_n^{(1)'} + iC_2 h_n^{(1)}}{C_1 \lambda h_n^{(2)'} + C_2 h_n^{(2)}} \right] P_n(\cos \theta) d\xi \quad (6.1)
 \end{aligned}$$

where C_1 and C_2 are given on p. 10.

Unfortunately, the order of summation and integration in (6.1) cannot be interchanged, i.e. the total pressure cannot be found as the sum of the pressures associated with the

individual vibrational modes. This can be seen for the specific case $r = 1$, $\tau = -\lambda$, and $\Theta = \pi$ as follows. At the moment of impact, $\tau = -\lambda$, we have for each mode and for all Θ , $v_n = w_n$

$$= \frac{\partial^2 v_n}{\partial t^2} = \frac{\partial^2 w_n}{\partial t^2} = 0.$$
 Our equations of equilibrium, (2.9) and (2.10) require that the pressure at the surface of the sphere must likewise vanish for each mode at $\tau = -\lambda$, so that the total pressure would be zero for all Θ . We should expect however, from what is known of the theory of scattering of plane waves, that the pressure Q_0 would be doubled for $\Theta = \pi$ and not reduced to zero.

Alternatively, we recall from p. 16 that the total radial acceleration is discontinuous at $\tau = -\lambda$, $\Theta = \pi$. Therefore the total pressure as summed mode by mode will be discontinuous, indicating the non-uniformity of convergence of the series in (6.1).

Because of this peculiarity in convergence, it is not possible to obtain an approximate solution for the pressure by considering just the first few terms of the series. $\bar{\psi}$, (4.15), must be found in closed form if P_{total} is to be evaluated. This has not as yet proved feasible because of the complexity of the summation which must be made. It was noted however that the expansions for $\bar{\psi}^0$ and $\bar{\psi}$ are very similar for $r = 1$, and ξ very large or $(\frac{\tau}{\lambda} - \cos \Theta)$ very small. This fact can be used to obtain the pressure at the surface of the sphere for $\tau/\lambda \approx \cos \Theta$.

By comparison with the expression for $\bar{\psi}_0$ on page 9 it is seen that the pressure associated with the incident wave may be written

$$P_I = Q_0 = -\frac{Q_0 i}{2\pi} \int_{-i\alpha\lambda-\infty}^{-i\alpha\lambda+\infty} \frac{e^{i\zeta\tau/\lambda}}{\zeta} \sum_{n=0}^{\infty} \delta_{jn}(\lambda\xi r) P_n(\cos \theta) (2n+1) (-i)^n d\zeta.$$

For $\zeta \gg \beta$ and $r = 1$, P_{II} (cf. 6.1) becomes, to first order

$$P_{II} = \frac{Q_0}{2\pi} \int_{-i}^{-i\alpha\lambda+\infty} \frac{e^{i\zeta\tau/\lambda}}{\zeta} \sum_{n=0}^{\infty} \frac{\sin(\zeta - \frac{n\pi}{2} - \frac{\pi}{2})}{\zeta} (2n+1) (-i)^n P_n(\cos \theta) d\zeta \quad (6.2)$$

and P_I reduces to

$$P_I = -\frac{Q_0 i}{2\pi} \int_{-i\alpha\lambda-\infty}^{-i\alpha\lambda+\infty} \frac{e^{i\zeta\tau/\lambda}}{\zeta} \sum_{n=0}^{\infty} \frac{\cos(\zeta - \frac{n\pi}{2} - \frac{\pi}{2})}{\zeta} (2n+1) (-i)^n P_n(\cos \theta) d\zeta. \quad (6.3)$$

Equations (6.4) and (4.14) tell us that

$$\zeta e^{-i\zeta \cos \theta} \xrightarrow{\zeta \rightarrow \infty} \sum_{n=0}^{\infty} \cos(\zeta - \frac{n\pi}{2} - \frac{\pi}{2}) (2n+1) (-i)^n P_n(\cos \theta).$$

Therefore, take

$$(\zeta - \frac{\pi}{2}) e^{-i(\zeta - \pi/2) \cos \theta} \xrightarrow{\zeta \rightarrow \infty} \sum_{n=0}^{\infty} \sin(\zeta - \frac{n\pi}{2} - \frac{\pi}{2}) (2n+1) (-i)^n P_n(\cos \theta)$$

so that to first order:

$$\begin{aligned} P_{II} &= \frac{Q_0}{2\pi} \int \frac{e^{i\zeta(\frac{\tau}{\lambda} - \cos \theta)}}{\zeta} e^{i\frac{\pi}{2} \cos \theta} d\zeta \\ &= Q_0 e^{i\frac{\pi}{2}(\cos \theta + 1)} \quad \text{for } 0 \leq (\frac{\tau}{\lambda} - \cos \theta) < .05 \\ &= 0 \quad \text{for } (\frac{\tau}{\lambda} - \cos \theta) < 0 \end{aligned} \quad (6.4)$$

Higher order terms may be obtained in the same way.

To second order:

$$\begin{aligned} P_{II} &= \frac{Q_0}{2\pi} \int \frac{e^{i\zeta\tau/\lambda}}{\zeta} \sum_{n=0}^{\infty} \left[\left(\sin(\zeta - \frac{n\pi}{2} - \frac{\pi}{2}) \left(1 - \frac{in(n+1)}{2\zeta^2} \right) \right. \right. \\ &\quad \left. \left. + \frac{e^{i(\zeta - \frac{n\pi}{2} - \frac{\pi}{2})} [2 + 2\beta + n(n+1)]}{2\zeta^2} \right) (2n+1) (-i)^n P_n d\zeta \right] \end{aligned}$$

$$= \frac{Q_0}{2\pi} \int \frac{e^{i\zeta\tau/\lambda}}{\zeta} \sum_{n=0}^{\infty} \left[\frac{\sin(\zeta - \frac{n\pi}{2} - \frac{\pi}{2})}{\zeta} + \frac{\cos(\zeta - \frac{n\pi}{2} - \frac{\pi}{2})n(n+1)}{2\zeta^2} \right. \\ \left. + \frac{\beta+1}{\zeta^2} e^{i(\zeta - \frac{n\pi}{2} - \frac{\pi}{2})} \right] (2n+1)(-1)^n P_n(\cos \theta) d\zeta \quad (6.5)$$

$$P_I = - \frac{Q_{0i}}{2\pi} \int \frac{e^{i\zeta\tau/\lambda}}{\zeta} \sum_{n=0}^{\infty} \left[\frac{\cos(\zeta - \frac{n\pi}{2} - \frac{\pi}{2})}{\zeta} - \frac{\sin(\zeta - \frac{n\pi}{2} - \frac{\pi}{2})n(n+1)}{2\zeta^2} \right] \\ \cdot (2n+1)(-1)^n P_n(\cos \theta) d\zeta. \quad (6.6)$$

In this case

$$e^{-i\zeta \cos \theta} \xrightarrow{\zeta \rightarrow \infty} \sum_{n=0}^{\infty} (2n+1)(-1)^n P_n(\cos \theta) \left[\frac{\cos(\zeta - \frac{n\pi}{2} - \frac{\pi}{2})}{\zeta} - \frac{\sin(\zeta - \frac{n\pi}{2} - \frac{\pi}{2})n(n+1)}{2\zeta^2} \right]$$

therefore by analogy, to second order:

$$e^{-i(\zeta - \frac{\pi}{2}) \cos \theta} \xrightarrow{\zeta \rightarrow \infty} \sum_{n=0}^{\infty} (2n+1)(-1)^n P_n \left[\frac{\sin(\zeta - \frac{n\pi}{2} - \frac{\pi}{2})}{\zeta} \left[1 + \frac{\pi}{2\zeta} \right] + \frac{\cos(\zeta - \frac{n\pi}{2} - \frac{\pi}{2})n(n+1)}{2\zeta^2} \right].$$

This does not correspond exactly to the first two terms in P_{II} , therefore we must subtract

$$\frac{\frac{\pi}{2} e^{-i(\zeta - \frac{\pi}{2}) \cos \theta}}{\zeta} \xrightarrow{\zeta \rightarrow \infty} \sum_{n=0}^{\infty} \frac{\pi}{2\zeta^2} \sin(\zeta - \frac{n\pi}{2} - \frac{\pi}{2}) (2n+1)(-1)^n P_n(\cos \theta).$$

We also have, again to second order

$$(\beta+1) \left[\frac{e^{-i\zeta \cos \theta}}{\zeta} + \frac{ie^{-i(\zeta - \frac{\pi}{2}) \cos \theta}}{\zeta} \right] \xrightarrow{\zeta \rightarrow \infty} (\beta+1) \sum_{n=0}^{\infty} \left[\frac{\cos(\zeta - \frac{n\pi}{2} - \frac{\pi}{2})}{\zeta^2} + \frac{i \sin(\zeta - \frac{n\pi}{2} - \frac{\pi}{2})}{\zeta^2} \right] (2n+1)(-1)^n P_n(\cos \theta).$$

P_{II} can now be written:

$$\begin{aligned}
 P_{II} &= \frac{Q_0}{2\pi} \int \frac{e^{i\zeta\tau/\lambda}}{\zeta} \left[e^{-i(\zeta - \pi/2)\cos\theta} - \frac{\pi}{2} \frac{e^{-i(\zeta - \frac{\pi}{2})\cos\theta}}{\zeta} \right. \\
 &\quad \left. + (\beta+1) \left(\frac{e^{-i\zeta\cos\theta}}{\zeta} + \frac{ie^{-i(\zeta - \frac{\pi}{2})\cos\theta}}{\zeta} \right) \right] d\zeta \\
 P_{II} &= \frac{Q_0}{2\pi} \int \frac{e^{i\zeta(\frac{\tau}{\lambda} - \cos\theta)}}{\zeta} \left[e^{i\frac{\pi}{2}\cos\theta} + \frac{\beta+1}{\zeta} (1 + ie^{i\frac{\pi}{2}\cos\theta}) \right. \\
 &\quad \left. - \frac{\pi}{2\zeta} e^{i\frac{\pi}{2}\cos\theta} \right] \\
 &= Q_0 \left[e^{i\frac{\pi}{2}(\cos\theta + 1)} - \left(\frac{\tau}{\lambda} - \cos\theta \right) (1+\beta) (1 + e^{i\frac{\pi}{2}(\cos\theta + 1)}) \right. \\
 &\quad \left. + \frac{\pi}{2} \left(\frac{\tau}{\lambda} - \cos\theta \right) e^{i\frac{\pi}{2}\cos\theta} \right] \quad \text{for } 0 \leq \left(\frac{\tau}{\lambda} - \cos\theta \right) << .05 \\
 &= 0 \quad \text{for } \left(\frac{\tau}{\lambda} - \cos\theta \right) < 0. \quad (6.7)
 \end{aligned}$$

Additional terms will be of little value since our expansion is valid only for $\zeta \gg \beta$, or $(\tau/\lambda - \cos\theta) << .05$. The terms we have found so far however are sufficient to tell us some things of importance.

The incoming wave will reach the point $(1, \theta)$ on the sphere at time $\tau/\lambda = \cos\theta$. The initial pressure for each θ is given by⁶

-
6. The elastic waves in the shell will travel more rapidly than the acoustic waves and will result in a pressure, $P \neq 0$, at $(1, \theta)$ before the time $\tau/\lambda = \cos\theta$, $\theta \neq \pi$. However, this effect is negligibly small compared with the one we are considering.

$$\begin{aligned}
 P_{\text{total}} &= P_I + \text{Re}P_{II} \\
 &= Q_0 + Q_0 \left\{ \cos\left(\frac{\pi}{2}(\cos \theta + 1)\right) - 18\left[\frac{\pi}{\lambda} - \cos \theta\right][1 + \cos\left(\frac{\pi}{2}(\cos \theta + 1)\right)] \right. \\
 &\quad \left. + \frac{\pi}{2}\left[\frac{\pi}{\lambda} - \cos \theta\right][\cos\left(\frac{\pi}{2} \cos \theta\right)] \right\}. \quad (6.8) \\
 &= Q_0 + Q_0 \cos\left[\frac{\pi}{2}(\cos \theta + 1)\right]. \quad (6.9)
 \end{aligned}$$

At $\theta = \pi$, the outermost point of the sphere, the first effect is that of a plane wave hitting a rigid wall so that we have

$$P_{II} = P_I; \quad P_{\text{total}} = 2Q_0.$$

At $\theta = \pi/2$, the wave just grazes the sphere and therefore

$$P_{II} = 0; \quad P_{\text{total}} = Q_0.$$

As θ varies from π to $\pi/2$, the initial pressure varies continuously from $2Q_0$ to Q_0 .

If the sphere were rigid, the steady state pressure distribution would be given by

$$P_{\text{total}} = P_I \quad 0 \leq \theta \leq \pi. \quad [5]$$

The results of section V indicate that we will have asymptotic values of $RQ_0/2$ for the stresses and zero for the radial acceleration, which also correspond to a uniform pressure of $Q_0 = P_I$.

At present, this is about all that can be said on the subject of the pressure distribution. A completely satisfactory way of dealing with the problem will not be had until it is possible to find the sum in (6.1).

VII. Conclusions.

Both the stress and the acceleration for each mode can readily be computed to any desired accuracy. For the stress, the zeroth mode is by far the most important and this is closely approximated by the zeroth mode of a simple quasi-static system (p. 18). The acceleration on impact of the outermost portion of the shell ($\theta = \pi$) can be found exactly and is seen to differ markedly from the accelerations associated with the individual vibrational modes.

The problem here considered, apart from its intrinsic interest, should serve as a valuable guide in the solution of similar problems involving obstacles of more complicated shape.

Bibliography

- [1] G. F. Carrier, "The Interaction of an Acoustic Wave and an Elastic Cylindrical Shell". Brown University report to the Office of Naval Research under Contract N7onr-35810, No. B11-4 (1951).
- [2] J. H. Jellett, "On the Properties of Extensible Surfaces". Roy. Irish Acad. Trans., Vol. 22, Part V, (1855).
- [3] S. Timoshenko, "Theory of Plates and Shells". 1st ed., McGraw-Hill, New York and London (1940).
- [4] H. Lamb, "On the Vibrations of a Spherical Shell". Proc. Lond. Math. Soc. 14, 50 (1883).
- [5] P. Morse, "Vibrations and Sound". McGraw-Hill, New York and London (1936).
- [6] R. D. Mindlin and H. H. Bleich, "Response of an Elastic Cylindrical Shell to a Transverse, Step Shock Wave". Columbia University report to the Office of Naval Research under Contract Nonr-266(08), No. 3 and Contract Nonr-266(09), No. 2; (1952).

Results to be Approximated

$\frac{\tau}{\lambda} + 1$	$\frac{-4Eh}{Q_0 R^2} \frac{\partial^2 w_0}{\partial \tau^2}$
0	0
.1	0.176
.2	0.180
.3	0.155

Results Obtained by Power Series Expansion

Terms used $\frac{\tau}{\lambda} + 1$	1	2	3	4	5	6	7	8	9	10	11	12
0	0	0	0	0	0	0	0	0	0	0	0	0
.1	0.4	0.04	0.239	0.157	0.184	0.177	0.178	0.178	0.178	0.178	0.178	0.178
.2	0.8	-0.64	0.955	-0.367	0.510	0.025	0.255	0.160	0.195	0.183	0.187	0.186
.3	1.2	-2.04	3.342	-3.350	3.308	-2.213	1.711	-0.729	0.620	-0.051	0.252	0.126

Table 1. Approximating the zeroth mode acceleration by a power series expansion.

(a)

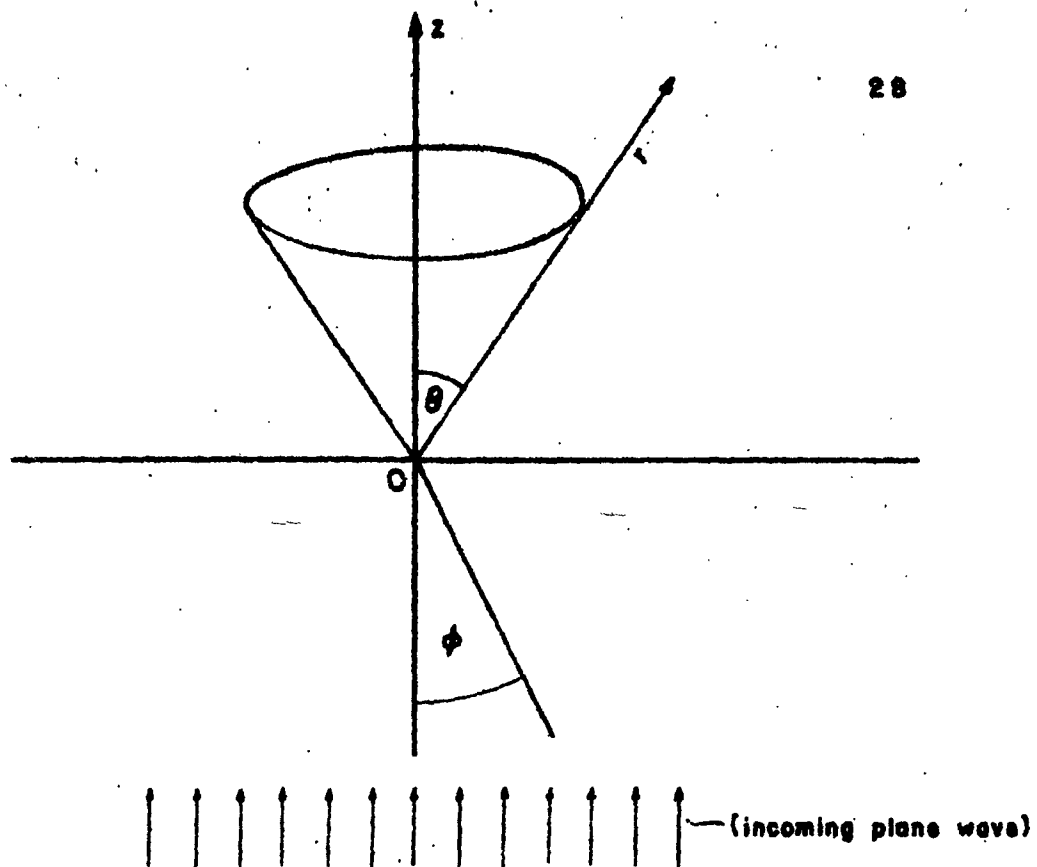
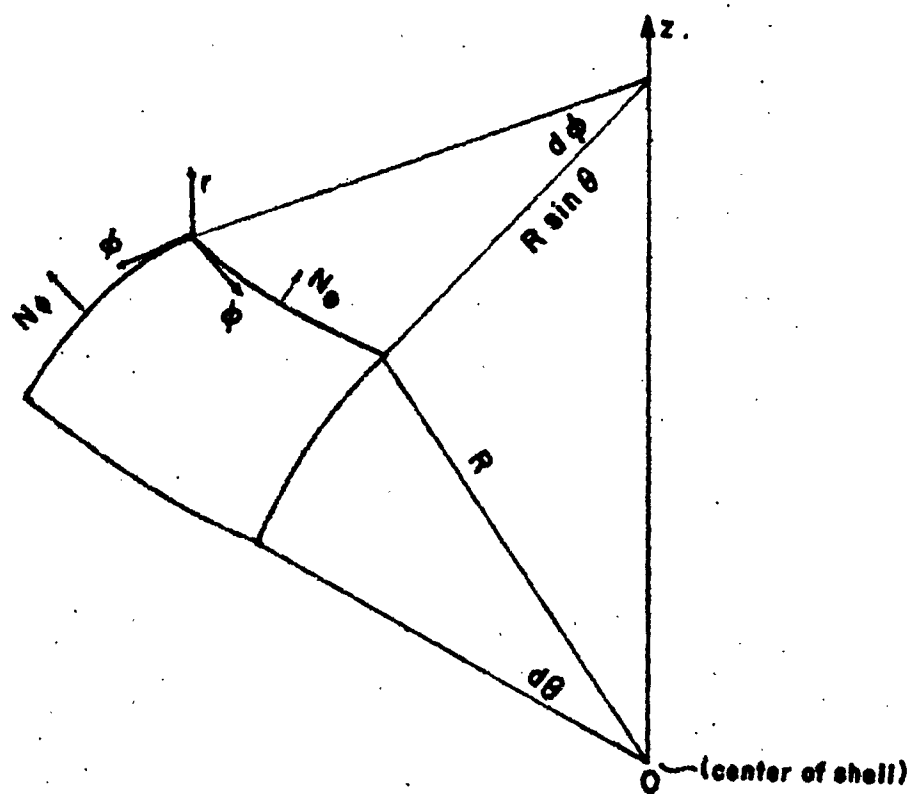


Fig. 1. Geometry of the problem.

(b)



BII-II

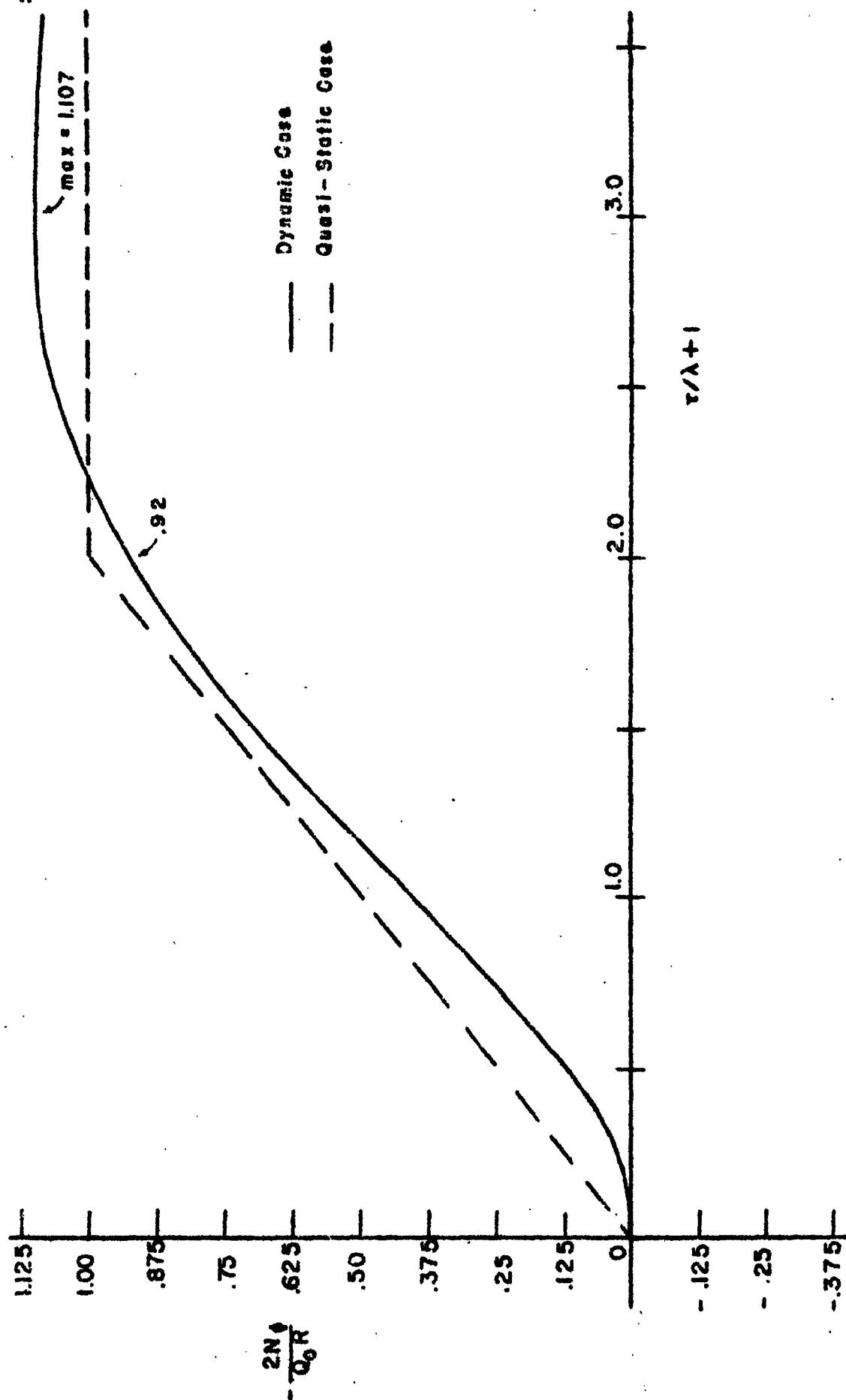


Fig. 2. Hoop stress for the zeroth mode.

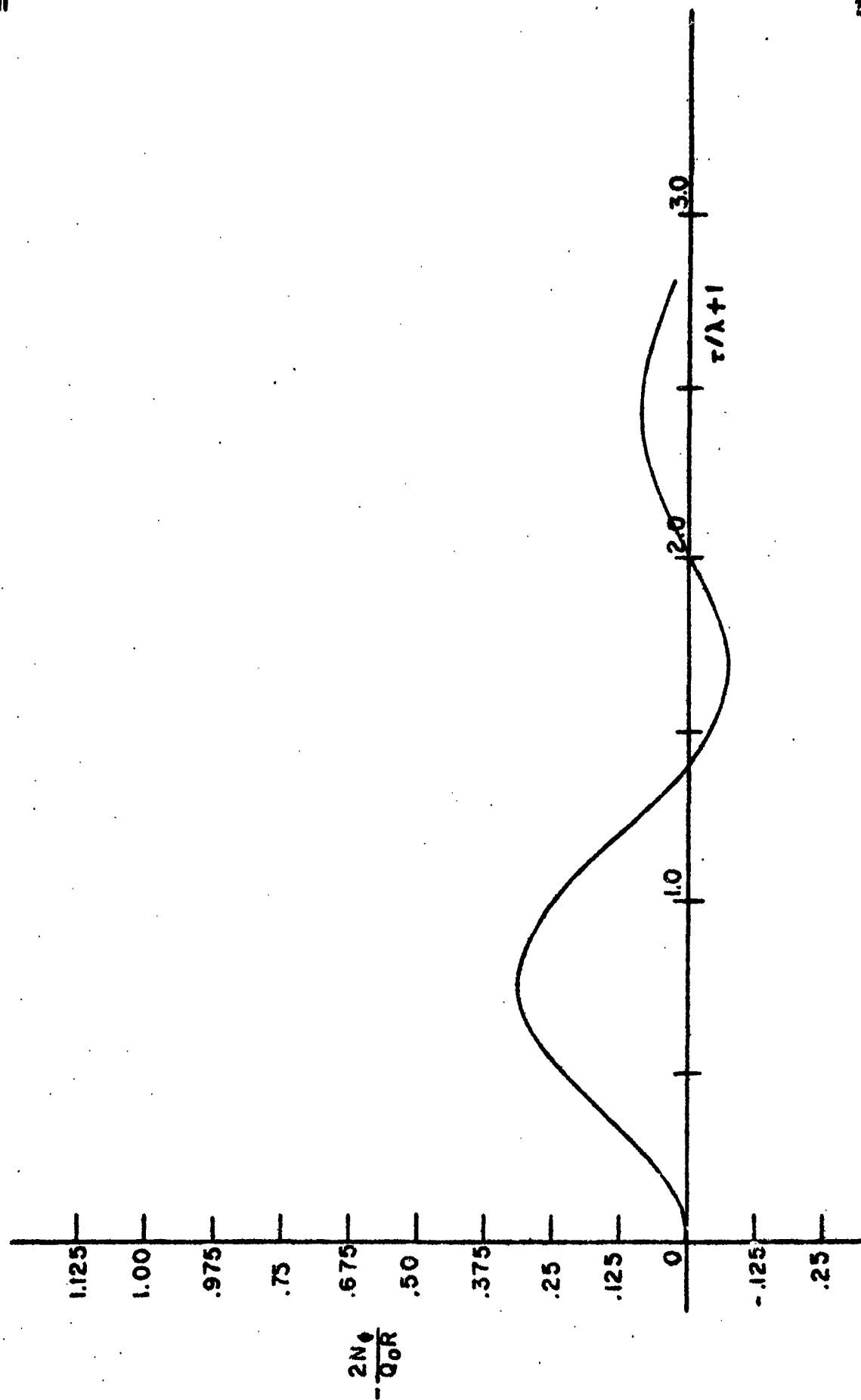


Fig. 3. Hoop stress for the first mode at $\theta = \pi$

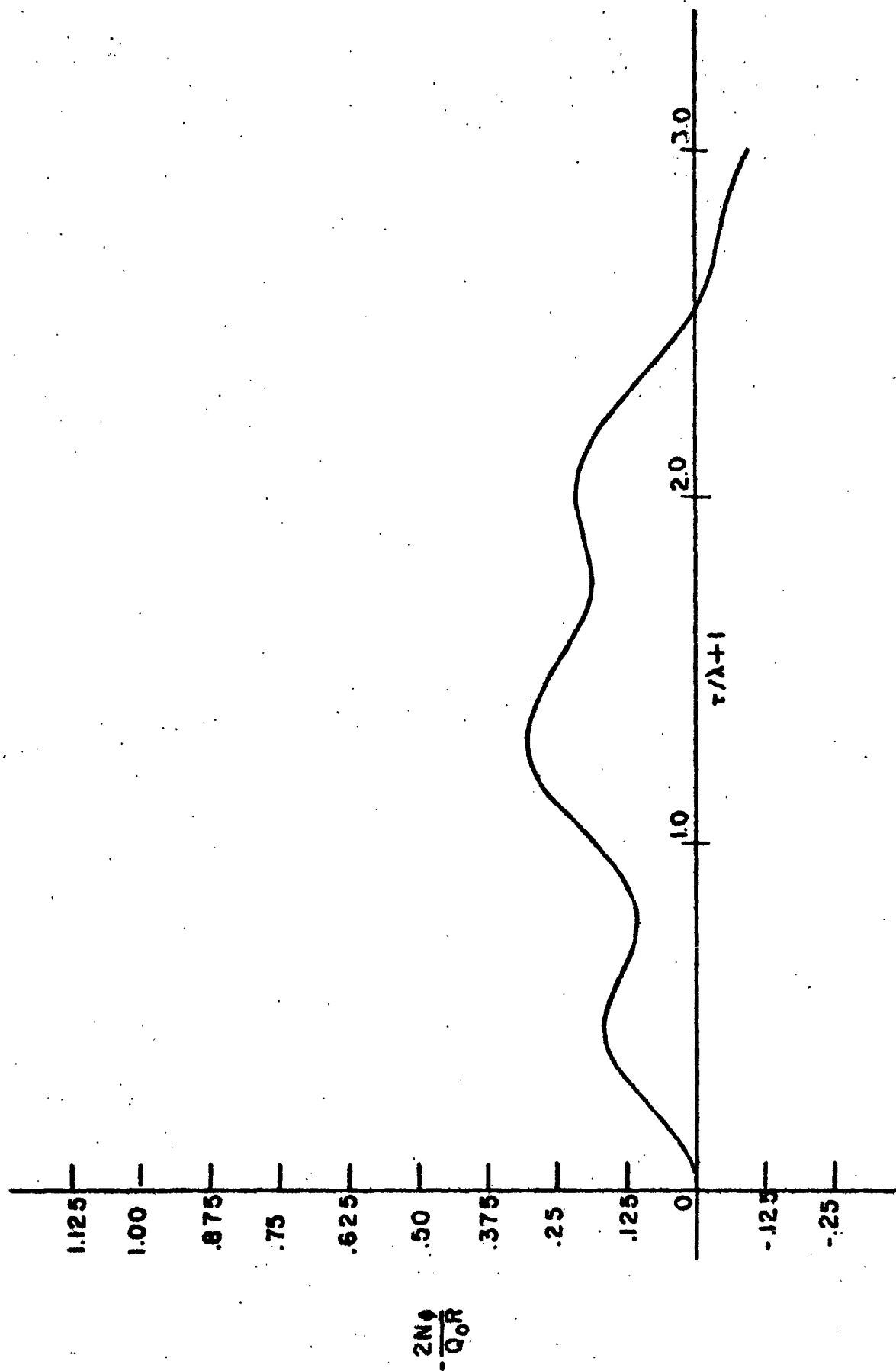


Fig. 4. Hoop stress for the second mode at $\theta = \pi$

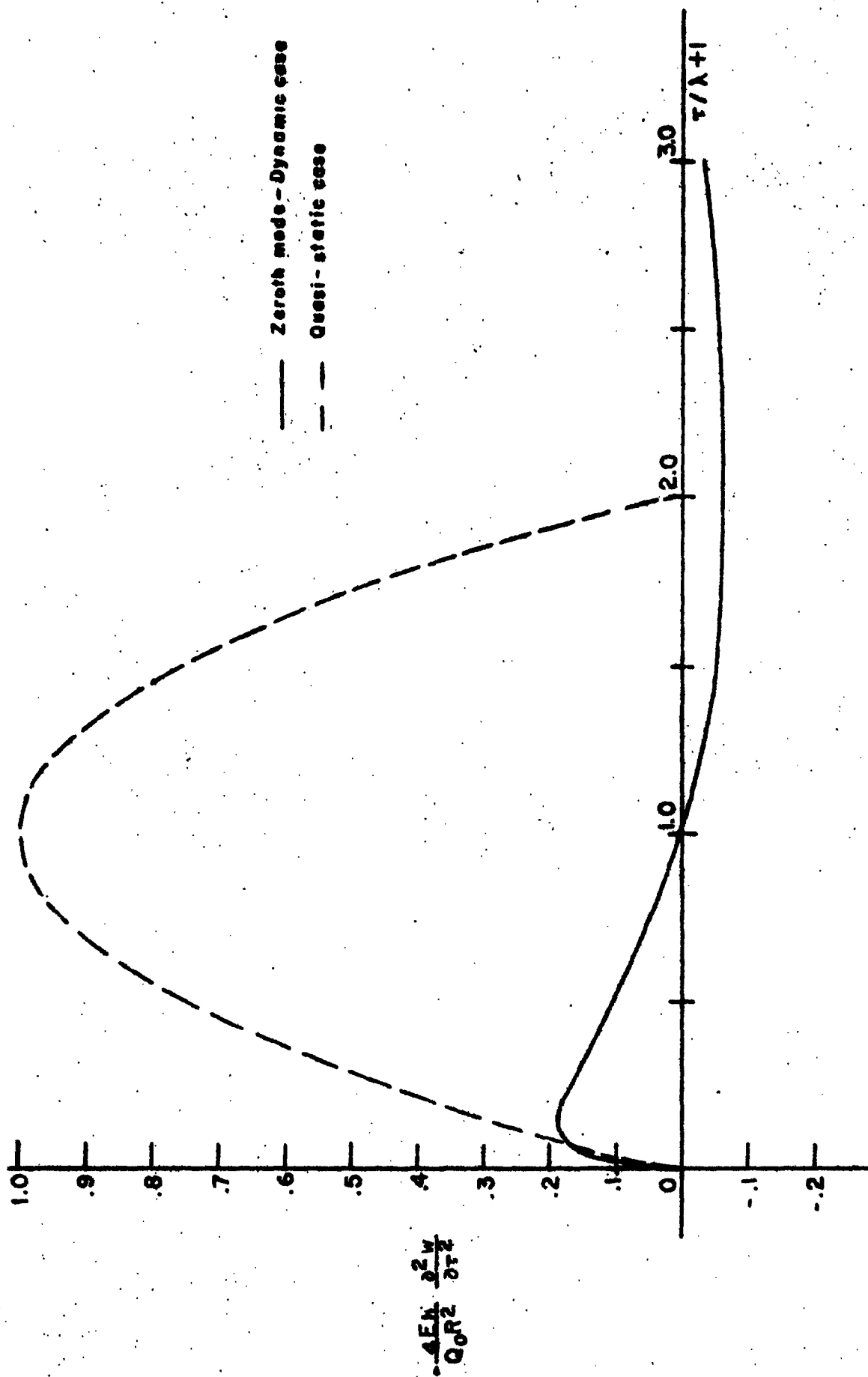


Fig. 5. Radial acceleration for the zeroth mode.

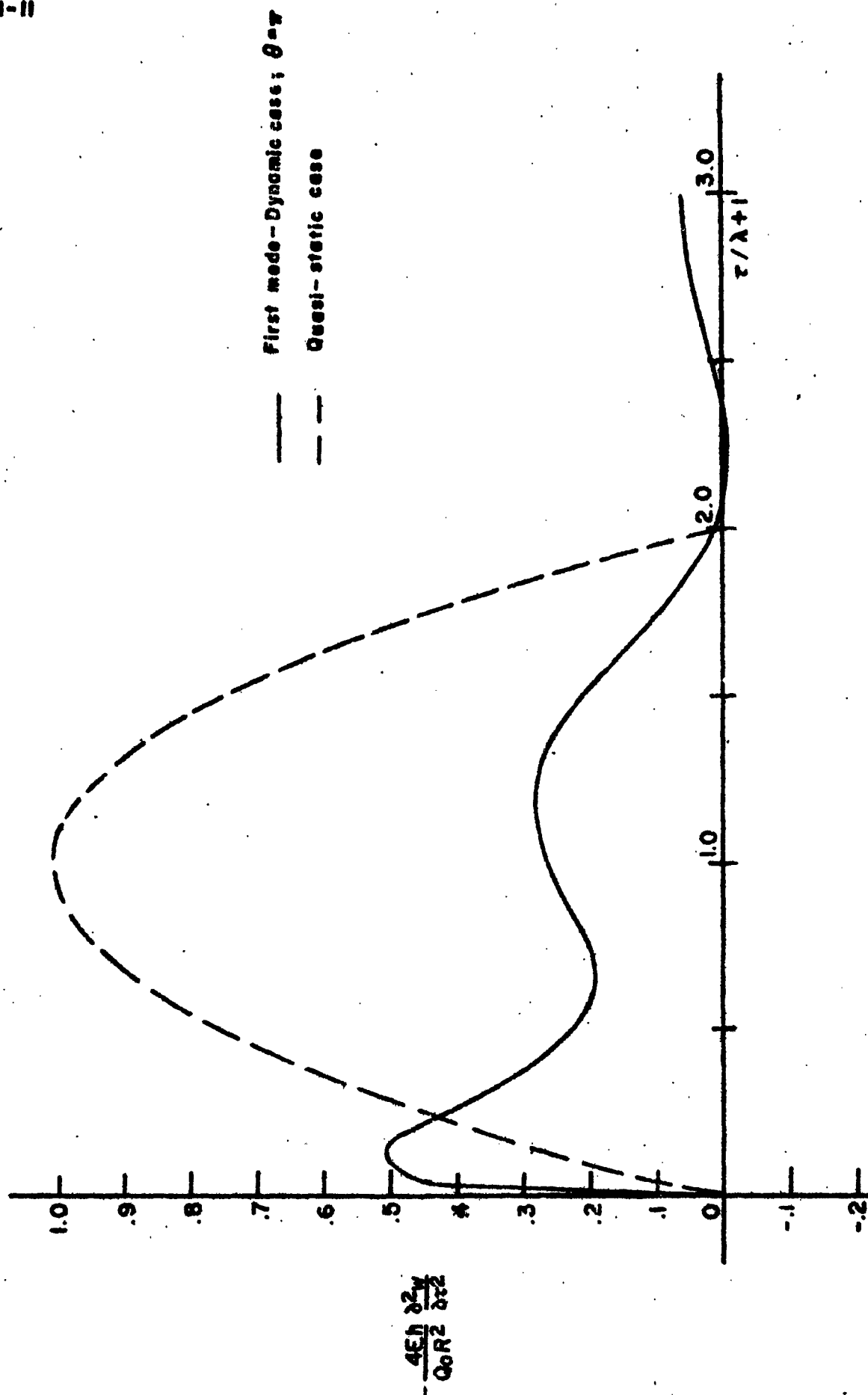


Fig. 6. Radial acceleration for the first mode at $\theta = \pi$

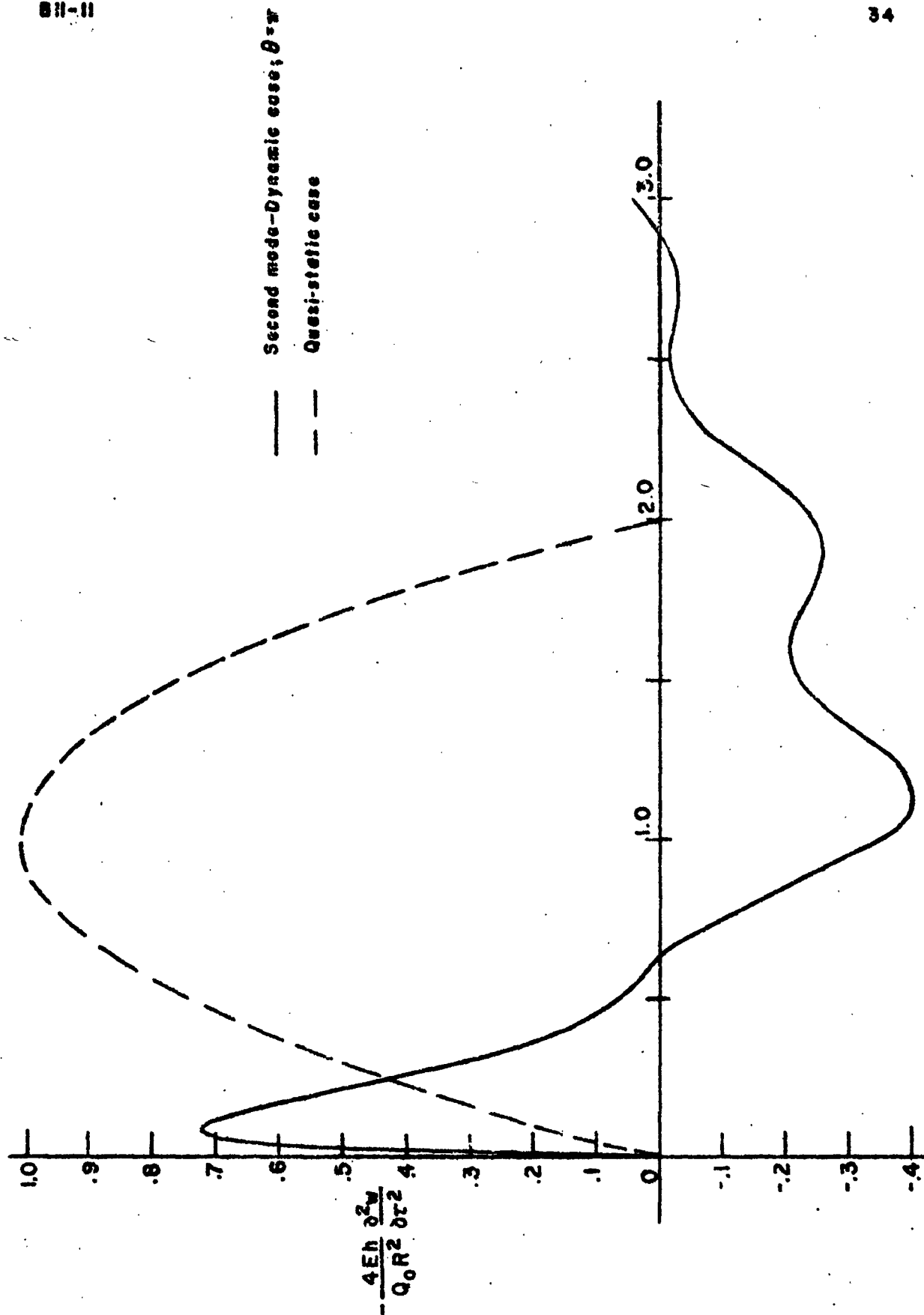


Fig. 7. Radial acceleration for the second mode at $\theta = \pi$

Distribution List
for
Technical and Final Reports Issued Under
Office of Naval Research Project NR-360-364, Contract N7onr-35810

I: Administrative, Reference and Liaison Activities of ONR

Chief of Naval Research Department of the Navy Washington 25, D. C. Attn: Code 438 (2) Code 432 (1) Code 466(via Code 108) (1)	Commanding Officer Office of Naval Research Branch Office 1000 Geary Street San Francisco, California (1)
Director, Naval Research Lab. Washington 25, D. C. Attn: Tech. Info. Officer (9) Technical Library (1) Mechanics Division (2)	Commanding Officer Office of Naval Research Branch Office 1030 Green Street Pasadena, California (1)
Commanding Officer Office of Naval Research Branch Office 495 Summer Street Boston 10, Massachusetts (2)	Officer in Charge Office of Naval Research Branch Office, London Navy No. 100 FPO, New York, N. Y. (5)
Commanding Officer Office of Naval Research Branch Office 346 Broadway New York 13, New York (1)	Library of Congress Washington 25, D. C. Attn: Navy Research Section (2)
	Commanding Officer Office of Naval Research Branch Office 844 N. Rush Street Chicago 11, Illinois (1)

II: Department of Defense and other interested Government Activities

a) General

Research & Development Board
Department of Defense
Pentagon Building
Washington 25, D. C.
Attn: Library(Code 3D-1075) (1)

Armed Forces Special Weapons
Project
P. O. Box 2610
Washington, D. C.
Attn: Lt. Col. G. F. Blunda (2)

Joint Task Force 3
12 St. & Const. Ave., N.W.
(Temp. U)
Washington 25, D. C.
Attn: Major B. D. Jones (1)

b) Army

Chief of Staff
Department of the Army
Research & Development Division
Washington 25, D. C.
Attn: Chief of Res. & Dev. (1)

Office of the Chief of Engineers
Assistant Chief for Works
Department of the Army
Bldg. T-7, Gravelly Point
Washington 25, D. C.
Attn: Structural Branch
(R. L. Bloor) (1)

Engineering Research & Development
Laboratory
Fort Belvoir, Virginia
Attn: Structures Branch (1)

Distribution List

2

Army (cont.)

Office of the Chief of Engineers Asst. Chief for Military Construction Department of the Army Bldg. T-3, Gravelly Point Washington 25, D. C. Attn: Structures Branch (M. F. Carey) (1) Protective Construction Branch (I. O. Thornley)(1)	Chief of Bureau of Ships Department of the Navy Washington 25, D. C. Attn: Director of Research (2) Code 423 (1) Code 442 (1) Code 421 (1)
Office of the Chief of Engineers Asst. Chief for Military Operations Department of the Army Bldg. T-7, Gravelly Point Washington 25, D. C. Attn: Structures Development Branch (W. F. Woollard)(1)	Director, David Taylor Model Basin Department of the Navy Washington 7, D. C. Attn: Code 720, Structures Division (1) Code 740, Hi-Speed Dynamics Div. (1)
U. S. Army Waterways Experiment Station P. O. Box 631 Halls Ferry Road Vicksburg, Mississippi Attn: Col. H. J. Skidmore (1)	Commanding Officer Underwater Explosions Research Div. Code 290 Norfolk Naval Shipyard Portsmouth, Virginia (1)
The Commanding General Sandia Base, P. O. Box 5100 Albuquerque, New Mexico Attn: Col. Canterbury (1)	Commander Portsmouth Naval Shipyard Portsmouth, N. H. Attn: Design Division (1)
Operations Research Officer Department of the Army Ft. Lesley J. McNair Washington 25, D. C. Attn: Howard Brackney (1)	Director, Materials Laboratory New York Naval Shipyard Brooklyn 1, New York (1)
Office of Chief of Ordnance Office of Ordnance Research Department of the Army The Pentagon Annex #2 Washington 25, D. C. Attn: ORDTB-PS (1)	Chief of Bureau of Ordnance Department of the Navy Washington 25, D. C. Attn: Ad-3, Technical Library (1) Rec, P. H. Girouard (1)
Ballistics Research Laboratory Aberdeen Proving Ground Aberdeen, Maryland Attn: Dr. C. W. Lampson (1)	Naval Ordnance Laboratory White Oak, Maryland RFD 1, Silver Spring, Maryland Attn: Mechanics Division (1) Explosive Division (1) Mech. Evaluation Div. (1)
c) <u>Navy</u> Chief of Naval Operations Department of the Navy Washington 25, D. C. Attn: OP-31 (1) OP-363 (1)	Commander U. S. Naval Ordnance Test Station Inyokern, California Post Office - China Lake, Calif. Attn: Scientific Officer (1)
	Naval Ordnance Test Station Underwater Ordnance Division Pasadena, California Attn: Structures Division (1)

Distribution List

3

Navy (cont.)

Chief of Bureau of Aeronautics
Department of the Navy
Washington 25, D. C.
Attn: TD-41, Technical Library (1)

Chief of Bureau of Ships
Department of the Navy
Washington 25, D. C.
Attn: Code P-314 (1)
Code C-313 (1)

Officer in Charge
Naval Civil Engr. Research &
Evaluation Laboratory
Naval Station
Port Hueneme, California (1)

Superintendent
U. S. Naval Post Graduate School
Annapolis, Maryland (1)

d) Air Forces

Commanding General
U. S. Air Forces
The Pentagon
Washington 25, D. C.
Attn: Res. & Development Div. (1)

Deputy Chief of Staff, Operations
Air Targets Division
Headquarters, U. S. Air Forces
Washington 25, D. C.
Attn: AFOIN-T/PV (1)

Office of Air Research
Wright-Patterson Air Force Base
Dayton, Ohio
Attn: Chief, Applied Mechanics
Group (1)

e) Other Government Agencies

U. S. Atomic Energy Commission
Division of Research
Washington, D. C. (1)

Director, National Bureau of
Standards
Washington, D. C.
Attn: Dr. W. H. Ramberg (1)

Supplementary Distribution List

<u>Addressee</u>	<u>No. of Copies</u>	
	<u>Unclassified Reports</u>	<u>Classified Reports</u>
Professor Lynn Beedle Fritz Engineering Laboratory Lehigh University Bethlehem, Pennsylvania	1	-
Professor R. L. Bisplinghoff Dept. of Aeronautical Engineering Massachusetts Institute of Technology Cambridge 39, Massachusetts	1	1
Professor Hans Bleich Dept. of Civil Engineering Columbia University Broadway at 117th St. New York 27, N. Y.	1	1

Distribution List

4

Addressee	<u>Unclassified Reports</u>	<u>Classified Reports</u>
Professor B. A. Boley Dept. of Aeronautical Engineering Ohio State University Columbus, Ohio	1	-
Professor G. F. Carrier Graduate Division of Applied Mathematics Brown University Providence, R. I.	1	1
Professor R. J. Dolan Dept. of Theoretical & Applied Mechanics University of Illinois Urbana, Illinois	1	-
Professor Lloyd Donnell Department of Mechanics Illinois Institute of Technology Technology Center Chicago 16, Illinois	1	-
Professor A. C. Eringen Illinois Institute of Technology Department of Mechanics Technology Center Chicago 16, Illinois	1	-
Professor B. Fried Dept. of Mechanical Engineering Washington State College Pullman, Washington	1	-
Mr. Martin Goland Midwest Research Institute 4049 Pennsylvania Avenue Kansas City 2, Missouri	1	-
Dr. J. N. Goodier School of Engineering Stanford University Stanford, California	1	-
Professor R. M. Hermes College of Engineering University of Santa Clara Santa Clara, California	1	1
Professor R. J. Hansen Dept. of Civil & Sanitary Engineering Massachusetts Institute of Technology Cambridge 39, Massachusetts	1	1

Distribution List

5

Addressee	<u>Unclassified Reports</u>	<u>Classified Reports</u>
Professor M. Hetenyi Walter P. Murphy Professor Northwestern University Evanston, Illinois	1	-
Dr. N. J. Hoff, Head Department of Aeronautical Engineering & Applied Mechanics Polytechnic Institute of Brooklyn 99 Livingston Street Brooklyn 2, New York	1	1
Dr. J. H. Hollomon General Electric Research Laboratories 1 River Road Schenectady, New York	1	-
Dr. W. H. Hoppmann Department of Applied Mechanics Johns Hopkins University Baltimore, Maryland	1	1
Professor L. S. Jacobsen Department of Mechanical Engineering Stanford University Stanford, California	1	1
Professor J. Kempner Department of Aeronautical Engineering and Applied Mechanics Polytechnic Institute of Brooklyn 99 Livingston Street Brooklyn 2, New York	1	1
Professor George Lee Department of Aeronautical Engineering Rensselaer Polytechnic Institute Troy, New York	1	-
Professor Paul Lieber Department of Aeronautical Engineering Rensselaer Polytechnic Institute Troy, New York	1	1
Professor Glen Murphy, Head Department of Theoretical & Applied Mechanics Iowa State College Ames, Iowa	1	-
Professor N. M. Newmark Department of Civil Engineering University of Illinois Urbana, Illinois	1	1

Distribution List

6

Addressee	<u>Unclassified Reports</u>	<u>Classified Reports</u>
Professor Jesse Ormondroyd University of Michigan Ann Arbor, Michigan	1	-
Dr. W. Osgood Armour Research Institute Technology Center Chicago, Illinois	1	-
Dr. R. P. Petersen, Director Applied Physics Division Sandia Laboratory Albuquerque, New Mexico	1	1
Dr. A. Phillips School of Engineering Stanford University Stanford, California	1	-
Dr. W. Prager, Chairman Graduate Division of Applied Mathematics Brown University Providence 12, R. I.	1	1
Dr. S. Raynor Armour Research Foundation Illinois Institute of Technology Chicago, Illinois	1	-
Professor E. Reissner Department of Mathematics Massachusetts Institute of Technology Cambridge 39, Massachusetts	1	-
Professor M. A. Sadowsky Illinois Institute of Technology Technology Center Chicago 16, Illinois	1	-
Professor V. L. Salerno Department of Aeronautical Engineering Rensselaer Polytechnic Institute Troy, New York	1	1
Professor M. G. Salvadori Department of Civil Engineering Columbia University Broadway at 117th Street New York 27, New York	1	-
Professor J. E. Stallmeyer Talbot Laboratory Department of Civil Engineering University of Illinois Urbana, Illinois	1	1

Distribution List

7

Addressee	<u>Unclassified Reports</u>	<u>Classified Reports</u>
Professor E. Sternberg Illinois Institute of Technology Technology Center Chicago 16, Illinois	1	-
Professor R. G. Sturm Purdue University Lafayette, Indiana	1	-
Professor F. K. Teichmann Department of Aeronautical Engineering New York University University Heights, Bronx New York, N. Y.	1	-
Professor C. T. Wang Department of Aeronautical Engineering New York University University Heights, Bronx New York, N. Y.	1	-
Project Files	2	2
Project Staff	5	-
For possible future distribution by the University	10	-
To ONR Code 438, for possible future distribution	-	10